Estimation of the error of the algorithm for reconstructing the reflection coefficient of the Earth surface on the example of images with the low atmospheric turbidity

V. V. Belov*[ab], M. V. Tarasenkov[ab]
[a] V.E. Zuev Institute of Atmospheric Optics Siberian Branch, Russian Academy of Sciences, 1, Academician Zuev Sq., Tomsk, 634021, Russia; [b] National Research Tomsk State University, 36 av. Lenina,Tomsk, 634050, Russia

ABSTRACT

An algorithm for atmospheric correction of satellite images combining the consideration of the main factors influencing imaging and a number of techniques allowing the computational time to be decreased considerably is analyzed. On the example of a series of images of the South of the Tomsk Region recorded from 7/13/2013 to 7/17/2013 with the low atmospheric turbidity, a comparison of the results of atmospheric correction using the suggested algorithm with the results obtained using the NASA MOD09 algorithm is performed. The correction error is estimated under assumption of a linear change of the reflection coefficient from image to image. Our comparison demonstrates that the results of correction differ within the correction error.

Keywords: atmospheric correction, Monte Carlo method, Earth surface reflection coefficient

1. INTRODUCTION

Information on the reflection coefficient of the Earth surface in the visible and near-IR ranges has a wide application when solving such problems as estimation of the state of forests and farmlands, extraction of mineral resources, climatic problems, etc. [1–4]. At present the application of passive satellite systems is one of the main methods of obtaining this information. However, their application has specificity. The atmosphere being the turbid medium influences on the solar radiation, and hence the received signal comprised not only light fluxes reflected from the observed regions of the Earth surface, but also background scattered radiation. For high atmospheric turbidity (fogs, aerosol smokes, etc.), the contribution of background radiation can be considerable or even exceed the useful signal. Elimination of this component from the received signal is called atmospheric correction. Without atmospheric correction, the reconstructed Earth surface reflection coefficient can have considerable error.

The problem of atmospheric correction of satellite images has been solved for several decades. At present there are several approaches to the solution of this problem, for example [5–10]. However, each of the existing approaches has restrictions. To take into account all factors influencing on imaging in the visible and UV ranges, the atmospheric correction algorithm was developed described in [11–13]. In the present work, the errors in reconstruction of the reflection coefficient by the suggested algorithm and by the standard NASA MOD09 algorithm [6] are considered. A comparison is performed for images of the test region of the South of the Tomsk Region 100 × 100 km for the period from 7/13/2013 to 7/17/2013.

Problem formulation and sources of initial data

The problem of reconstruction of distribution of the Earth surface reflection coefficients is formulated as follows (Fig. 1). The spherical atmosphere – Earth surface system is considered. The model of the stratified atmosphere is assigned by a set of spherical homogeneous layers. The Earth surface represents the Lambertian surface with unknown distribution of the reflection coefficient. The passive satellite system oriented in the direction $\boldsymbol{\omega}_{\mathrm{d}}$ is situated at the altitude hd from the surface. Observations of the Earth surface within the preset field-of-view angle are performed. Let the spatial resolution of the optical receiver forming the image be constant in the observation region. A parallel flux of sunlight is incident on the upper atmospheric boundary in the direction $\boldsymbol{\omega}_{\mathrm{sun}}$. It is required, knowing the optical atmospheric parameters and the signal intensity measured by the satellite system, to reconstruct the distribution of the reflection coefficient over the observed Earth surface region.

21st International Symposium on Atmospheric and Ocean Optics: Atmospheric Physics, edited by G. G. Matvienko, O. A. Romanovskii, Proc. of SPIE Vol. 9680, 96801Q

As the initial intensities measured by the satellite system, the data of the MODIS device with spatial resolution of 500 m in the nadir were taken [14]. The aerosol optical thickness (AOT) of the atmosphere measured by the AERONET system [15] and the satellite data on the temperature and pressure profiles [14] obtained using the MODIS device were taken as the initial optical model of the atmosphere. The atmospheric correction was carried out only for cloudless fragments. The cloud fragments were eliminated from calculations using the cloud mask [14] obtained using the MODIS device.

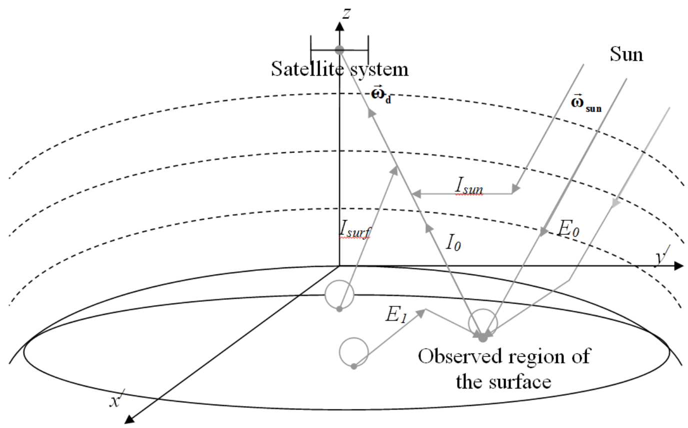

Figure 1 – Geometry of the problem being solved.

Knowing the AOT of the Earth surface fragment for which the atmospheric correction was performed at the moment of satellite measurements, among the LOWTRAN-7 models [16] we took the model that had the closest AOT value. The aerosol parameters of the atmosphere were assigned according to this model. The vertical profile of the molecular scattering coefficient was calculated from the formula [17]

$$\sigma_{s,m}(z) = \sigma_{s,m}^{(0)} \frac{P(z)}{P_0} \cdot \frac{T_0}{T(z)}, \tag{1}$$

where $\sigma_{s,m}$ is the molecular scattering coefficient at altitude z, in km–1, $\sigma_{s,m}^{(0)}$ is the molecular scattering coefficient at the wavelength λ, temperature $T_0 = 288.15$ K, and pressure $P_0 = 1013.25$ mb; P and T are the air temperature and pressure at the given altitude retrieved from the satellite data.

The vertical profile of the molecular absorption coefficient was chosen from the LOWTRAN-7 models.

Atmospheric correction algorithm

The algorithm for the atmospheric correction and the program complex developed on its basis were considered in [11–13]. The algorithm was based on the radiative transfer equation. The signal received by the satellite system (Fig. 1) comprised solar haze radiation I_{sun} – solar radiation scattered in the atmosphere and non-interacted with the Earth surface, unscattered radiation I0 reflected from the observed region of the Earth surface, and surface light haze radiation I_{surf} – scattered radiation reflected from the Earth surface. Thus, for each observation point on the surface we can write [11]

$$I_{sum}(x_w, y_w) = I_0(x_w, y_w) + I_{sun}(x_w, y_w) + I_{surf}(x_w, y_w), \tag{2}$$

where

$$I_0(x_w, y_w) = \frac{r_{surf}(x_w, y_w) E_{sum}(x_w, y_w) \mu(x_w, y_w)}{\pi} \exp\left(-\tau(x_w, y_w)\right), \tag{3}$$

$$I_{surf}(x_w, y_w) = \iint_S r_{surf}(x'_w, y'_w) E_{sum}(x'_w, y'_w) h(x'_w, y'_w, x_w, y_w) dx'_w dy'_w . \tag{4}$$

Here r_{surf} specifies the distribution of the reflection coefficient over the Earth surface, E_{sum} is the distribution of the total irradiance over the Earth surface, τ is the optical length of the path from the point on the surface to the satellite system, (x_w, y_w) are surface coordinates of a certain observation point, $h(\bullet)$ is the point spread function (PSF) of the channel of forming the adjacency effect, S denotes the entire spherical Earth surface, (x'_w, y'_w) are the surface coordinates of the points over which integration is conducted, μ is the cosine of the angle between the direction to the receiver and the vertical at the observation point.

Based on the analysis performed in [11], the total irradiance of the Earth surface is formed mainly by directly transmitted and diffuse solar radiation components as well as by singly scattered radiation. Therefore, the total irradiance under assumption that the directly transmitted and diffuse solar radiation change slightly is approximately equal to

$$E_{sum}(x_w, y_w) \approx E_0 + E_0 \iint_S r_{surf}(x'_w, y'_w) h_1(x'_w - x_w, y'_w - y_w) dx'_w dy'_w, \tag{5}$$

where E_0 is the Earth irradiance by direct and diffuse solar radiation and $h_1(\bullet)$ is the PSF of the channel of forming the additional irradiance of the Earth surface due to re-reflection.

Then under assumption that the reflection coefficient does not change within the pixel, from Eqs. (2)–(5) we derive the system of linear equations for $Q = r_{surf} E_{sum}$ [11]:

$$\begin{cases} I_{sum}(x_{w,1}, y_{w,1}) - I_{sun}(x_{w,1}, y_{w,1}) = \dfrac{Q_1 \mu_1}{\pi} \exp(-\tau_1) + \sum\limits_{k=1}^{N} Q_k H_{k,1} \\ \cdots \\ I_{sum}(x_{w,N}, y_{w,N}) - I_{sun}(x_{w,N}, y_{w,N}) = \dfrac{Q_N \mu_N}{\pi} \exp(-\tau_N) + \sum\limits_{k=1}^{N} Q_k H_{k,N} \end{cases} \tag{6}$$

where $H_{k,i}$ is the integral PSF of forming the adjacency effect over the area of the k-th pixel during observation of the i-th pixel.

Knowing Q, the reflection coefficient $\tilde{r}_{surf}$ with allowance for the first order re-reflection is determined by the nonlinear system of the form [11]:

$$\begin{cases} \dfrac{Q_1}{E_0} = \tilde{r}_{surf,1} \cdot \left(1 + \sum\limits_{l=1}^{N} \tilde{r}_{surf,l} \cdot P_l\right) \\ \ldots \\ \dfrac{Q_N}{E_0} = \tilde{r}_{surf,N} \cdot \left(1 + \sum\limits_{l=1}^{N} \tilde{r}_{surf,l} \cdot P_l\right) \end{cases} \tag{7}$$

where P_l is the integral PSF of the channel of forming additional irradiance of the l-th pixel surface.

The other multiplicities of re-reflection can be taken into account using the formula [11]:

$$r_{surf,i} \approx \frac{\tilde{r}_{surf,i}\left(1 + \tilde{r}_{surf,i}\gamma_1\right)}{1 + \tilde{r}_{surf,i}\gamma_1\left(1 + \tilde{r}_{surf,i}\gamma_1\right)}, \tag{8}$$

where r_{surf} is the reflection coefficient reconstructed with allowance for all multiplicities of re-reflection, γ_1 describes the contribution of singly re-reflected radiation to the Earth surface irradiance in the homogeneous case.

To obtain the solution, it is necessary to calculate I_{sun}, E_0, H, P, and γ_1. These quantities were calculated by the Monte Carlo method [18–20]. The above-described algorithms were tested in [11, 20]. In [11–13], a number of techniques were suggested that accelerated obtaining of results.

The first of them is the use of the approximation formulas for the solar haze intensity [11–13]. This formula allows calculation to be performed only for a set of central points rather than for each pixel and to reconstruct the results at all intermediate points.

The second technique consists in the construction of isoplanarity zones [11–13]. The matter is that the function $h(\bullet)$ changes from one pixel to another, but it is possible to select the isoplanarity zones where the PSF of the channel of forming the adjacency effect can be considered approximately constant; then it is possible to consider that the function $h_1(\bullet)$ is independent of the arrangement of the pixel relative to the receiving system.

The third technique is the introduction of radii of the adjacency effect and re-reflection formation [11–13]. The radius of the adjacency effect is the radius of the area on the Earth surface within which Isurf is mainly formed. The boundary of this area was chosen so that the error in determining Q with allowance for the surface haze did not exceed the preset level (in calculations, it was 5 %). The expression for Q is given, for example, in [11]. The radius of forming the regions with additional irradiance E_1 caused by the process of re-reflection is determined analogously. The boundary of this area was chosen so that the error in determining the reflection coefficient with allowance for the additional irradiance did not exceed the preset value (in calculations it was 5 %). The expression for this radius is given, for example, in [11].

Closed calculation performed in [11] demonstrated that the use of the suggested techniques decreased the computational time 6 folds. Test comparisons also demonstrated that the adjacency effect and re-reflections in the visible range must be taken into account, especially for the highly turbid atmosphere.

Algorithm MOD09

The algorithm MOD09, according to [6], consists of several stages. In the beginning, the concentration of water vapor and the vertical profiles of the temperature and pressure are determined from the data of satellite AOT measurements as well as the model of the atmosphere is chosen based on measurements of the light intensity in several spectral ranges among the previously constructed models whose parameters are closest to the conditions of imaging. For this optical model, the problem of atmospheric correction is solved for each observed pixel separately under assumption that the surface is homogeneous. Then for each observed pixel the average reflection coefficient is calculated based on its values in the neighboring pixels. After that the correction procedure is performed considering the inhomogeneity of the reflection coefficient on the Earth surface. This correction is performed under assumption of isoplanarity of the entire image and a number of other assumptions which are not fulfilled for the highly turbid atmosphere. Results of atmospheric correction by the algorithm MOD09 in the electronic form can be found, for example, in [14].

Technique of estimating the error in atmospheric correction

In [12–13, 21] the reflection coefficients were reconstructed using the developed program complex. The estimation of the error in atmospheric correction is complicated by the fact that the true average value of the reflection coefficient for the observed fragment is not known. To bypass this problem, the error was estimated in [21] under assumption that the reflection coefficient for the considered time interval changes slightly, and it is possible to set it constant. In [7] a more successful approach was used. It was assumed that between measurements no considerable change of the reflection coefficient was observed, and it could be considered approximately linear. Then, having reflection coefficients for the $(i-1)$-th and $(i+1)$-th measurements, the reflection coefficient for the i-th measurement can be estimated from the formula [7]:

$$r^*_{surf,i} = \frac{(t_i - t_{i-1}) r_{surf,i+1} + (t_{i+1} - t_i) r_{surf,i-1}}{t_{i+1} - t_{i-1}}, \qquad (9)$$

where t_i is the time of the i-th measurement, $r^*_{surf,i}$ is the approximate estimate of the reflection coefficient from its values the day before and the day later, $r_{surf,i}$ is the reflection coefficient of the Earth surface reconstructed using the correction algorithm for the i-th day.

Then σ determined from the formula [7]

$$\sigma = \sqrt{\frac{\sum_{i=2}^{N-1} \frac{1}{t_{i+1} - t_{i-1}} \left(r_{surf,i}^{*} - r_{surf,i} \right)^2}{\sum_{i=2}^{N-1} \frac{1}{t_{i+1} - t_{i-1}}}}, \quad (10)$$

where N is the number of the examined images, can be considered as an estimate of the error in reconstructing the reflection coefficient for the given fragment of the Earth surface. It should be noted that satellite images at different times differed by spatial resolutions. To compare them, statistical data were averaged over the grid 1 km in latitude and longitude.

Estimation of the error in atmospheric correction

Let us consider the estimated error in atmospheric correction using the suggested algorithm and the algorithm MOD09. For an example, the fragment to the south of the Tomsk Region with coordinates 55.95–56.85° N and 84.05–84.95° E (100 × 100 km) was chosen for the period from 7/13/2013 to 7/17/2013 registered at wavelengths of 0.422, 0.469, 0.555, 0.645, and 1.24 μm. These days were chosen because the cloud cover index for them was less than 20 % and the data on the aerosol optical thickness (AOT) were available from the Station Tomsk-22 (56° N and 84° E) of the Aeronet System. The average error estimated by formula (10) for the examined fragment and the reflection coefficients for 5 MODIS channels retrieved by two algorithms are presented in Table 1. Figure 2 shows the average reflection coefficients for the examined images with allowance for σ_{aver}. Here σ_{aver} and $r_{surf,aver}$ at λ = 0.412 μm were not calculated by the algorithm MOD09, because for several images this algorithm gave non-physical results ($r_{surf} > 1$). As a whole, the comparison of the average values and the errors in estimating the reflection coefficients by the two algorithms demonstrated that the error of the algorithm MOD09 was slightly smaller. The differences in the average values were within the limits of the average variances. The results obtained by the suggested algorithm were slightly greater. This was most likely due to different atmospheric models. The variance for channel 5 was much smaller than the average. For channels 1, 3, and 4 the variance was only 2–3 times smaller than the average value of the reflection coefficient. For channel 8, the variance exceeded the average value of the reflection coefficient. Hence, the correction algorithm for this channel yielded unreliable results. The sources of high errors are the simplified model of the medium and the non-Lambertian reflecting surface [22].

Table 1. Average reflection coefficients $r_{surf,aver}$ and error σ_{aver} estimated by the suggested algorithm and the algorithm MOD09. Calculations were performed for 5 MODIS channels and 6 images of the test region.

Serial number of the channel	Wavelength, μm	Suggested algorithm		Algorithm MOD09	
		$r_{surf,aver}$	σ_{aver}	$r_{surf,aver}$	σ_{aver}
1	0.645	3.32E-02	1.40E-02	2.65E-02	1.32E-02
3	0.469	2.36E-02	1.00E-02	1.43E-02	7.11E-03
4	0.555	5.04E-02	2.19E-02	4.55E-02	2.12E-02
5	1.24	0.309	7.62E-02	0.272	6.48E-02
8	0.412	0.055491	8.03E-02	–	–

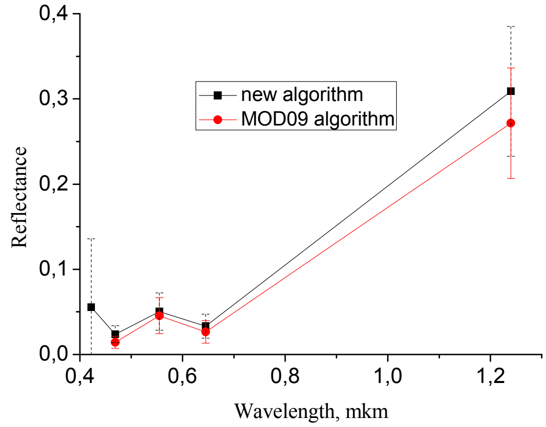

Fig. 2 – Comparison of the reflection coefficients averaged over the entire test region for the period from 7/13/2013 to 7/17/2013 calculated by two algorithms taking into account the average variance σ_{aver}.

Conclusions

The comparison of the suggested algorithm with the algorithm MOD09 demonstrated that the algorithm MOD09 was slightly better for low atmospheric turbidity. However, the difference between the results of algorithmic implementation was within the computational error. In future we plan to compare results of application of these two algorithms to images of the highly turbid atmosphere where the processes not considered by the algorithm MOD09 will give considerable contribution to the results. We also plan to improve the models of the medium used for correction in our future work and to consider the non-Lambertian surface.

This work was supported in part by the Russian Foundation for Basic Research (grants Nos. 15-01-00783-A and 15-07-06811-A), by the President of the Russian Federation under the Program for Support of Leading Scientific Schools NSh-4714.2014.5 and by the Tomsk State University Academician D. I. Mendeleev Scientific Fund Program (grant No. 8.1.27.2015 for 2015).

REFERENCES

[1] Varlamova E. V., and Solovyev V. S. “Study of NDVI variations in tundra and taiga areas of Eastern Siberia (Yakutia),” Atmos. Oceanic Optics, Papers 28(1), 64–67 (2015).
[2] Kozoderov V.V., Dmitriev E. V., Kamentsev V. P. “Cognitive technologies for processing optical images of high spatial and spectral resolution,” Atmos. Oceanic Optics, Papers 27(6), 558–565 (2014).
[3] Polishchuk Yu. M., Tokareva O. S. “The use of satellite images for ecological estimate of flare firing of gas at oil fields of Siberia,” Atmos. Oceanic Optics, Papers 27(07), 647-651 [in Russian] (2014)
[4] Malakhov D. V., Islamgulova A. F. “The quantitative interpretation of pasture image parametres: an experience of low and moderate spatial resolution remotely sensed data application,” Atmos. Oceanic Optics, Papers 27(07), 587–592 [in Russian] (2014).
[5] Protasov K. T., Busygin L. A., Belov V. V. “The method of transform histograms of brightness as well as wavelet-correction of satellite image atmospheric distortions,” Atmos. Oceanic Optics, Papers 23(02), 136–142 [in Russian] (2010).
[6] Vermote E. F., Vermeulen A. “Atmospheric correction algorithm: spectral reflectances (MOD09),” Algorithm Theoretical Background document, version 4.0. 1999, http://modis.gsfc.nasa.gov/atbd/atbd_nod08.pdf.
[7] Breon F.-M., Vermote E. “Correction of MODIS surface reflectance time series for BRDF effects,” Remote Sens. Envir. Papers 125, 1–9 (2012).
[8] Vermote E. F., Saleos N. Z. E., Justice C. O. “Atmospheric correction of MODIS data in the visible to middle infrared: first results,” Remote Sens. Envir. Papers 83, 97–111 (2002).

[9] Reinersman P. N., Carder K. L. “Monte Carlo simulation of the atmospheric point-spread function with an application to correction for the adjacency effect,” Appl. Opt. Papers 34(21), 4453–4471 (1995).
[10] Sei A. “Analysis of adjacency effects for two Lambertian half-surfaces,” Int. J. Remote Sens. Papers 28(8), 1873–1890 (2007).
[11] Belov V. V., Tarasenkov M. V. “On the accuracy and operation speed of RTM algorithms for atmospheric correction of satellite images in the visible and UV ranges,” Atmos. Oceanic Optics, Papers 27(1), 54–61 (2014).
[12] Tarasenkov M. V., Belov V. V. “Software package for reconstructing reflective properties of the Earth’s surface in the visible and UV ranges,” Atmos. Oceanic Optics, Papers 28(1), 89–94 (2015).
[13] Tarasenkov M. V., Belov V. V. “Atmospheric correction algorithm for satellite images of nonuniform Earth’s surface in the visible and UV ranges,” Zh. Vychisl. Tekhnol. Papers 19(3), 48–56 (2014).
[14] https://lpdaac.usgs.gov/data_access.
[15] http://aeronet.gsfc.nasa.gov/.
[16] Kneizys F. X., Shettle E. P., Anderson G. P., Abreu L. W., Chetwynd J. H., Selby J. E. A., Clough S. A., Gallery W. O. “User guide to LOWTRAN_7,” ARGL-TR-86-0177.ERP 2010 / Hansom AFB. MA 01731. 137 p.
[17] Bucholtz A. “Rayleigh-scattering calculations for the terrestrial atmosphere,” Appl. Opt. Papers 34(15), 2765–2773 (1995).
[18] Belov V. V., Tarasenkov M. V. “Statistical modeling of the point spread function in the spherical atmosphere and a criterion for detecting image isoplanarity zones,” Atmos. Oceanic Optics, Papers 23(6), 441–447 (2010).
[19] Belov V. V., Tarasenkov M. V. “Statistical modeling of the intensity of light fluxes reflected by the Earth’s spherical surface,” Atmos. Oceanic Optics, Papers 23(3), 197–203 (2010).
[20] Belov V. V., Tarasenkov M. V., Piskunov K. P. “Parametrical model of solar haze intensity in the visible and UV ranges of the spectrum,” Atmos. Oceanic Optics, Papers 23(04), 294–297 [in Russian] (2010).
[21] Belov V. V., Tarasenkov M. V. “Reconstruction of the Earth surface reflection coefficients in the visible and UV ranges for processing of satellite images,” Atmospheric and Oceanic Optics. Atmospheric Physics: Collection of Reports of XX International Symposium, Tomsk: Publishing House IOA SB RAS, B69–B73 (2014).
[22] Roujean J.-L., Leroy M., Deschamps P. Y. “A bidirectional reflectance model of the Earth’s surface for the correction of remote sensing data,” J. Geophys. Res. Papers 97(D18), 20455–20468 (1992).